Biocatalysis and Agricultural Biotechnology 19 (2019) 101127

Contents lists available at ScienceDirect

Biocatalysis and Agricultural Biotechnology

journal homepage: www.elsevier.com/locate/bab

Probing the biomolecular targets of azo colorant carcinogens towards purified wetland peroxidase-computational cum in vitro validation

Saipreethi P, Rameshpathy Manian*

School of Bio Sciences and Technology, Vellore Institute of Technology (VIT), India

ARTICLE INFO

Keywords:
Peroxidase
Computational docking
Azo dyes
Biodegradation
GC-MS
Streptomyces coelicolor

ABSTRACT

Azo dyes are attributed to be noxious to aquatic organisms impeding the endocrinal and metabolic phenomenon. Moreover, they are dwelled to exhibit carcinogenesis, teratogenesis and mutagenesis on humans and animals. Hence, this study explicitly targets on eradication of azo dye toxicity by microbial peroxidase as a robust tool. A novel peroxidase producing wetland isolate, *Streptomyces coelicolor* strain SPR7 was bioprospected. Computational prediction of chemical properties of synthetic azo dyes followed by molecular docking using Autodock software, to assess dock score, scrutinize binding site residues, binding mode and interactions between peroxidase and dyes viz. Diazin Green, Acid Red 2, Metanil Yellow, Basic Blue 9, Orange-G and Eriochrome Black T were achieved. Out of all the dyes, Eriochrome Black T prophesied the highest negative binding energy (-7.2 kJ/mol) and was further selected for biodegradation strategies by purified peroxidase, with molecular mass of 45 kDa. The purified peroxidase evinced a higher decolorization rate (94.21%) of Eriochrome Black T (100 ppm). Docking results of interaction between dye and peroxidase were corroborative with degradation percentage. UV–vis spectroscopy, HPLC, FTIR and GC–MS were performed for validating the biotransformation strategy. Moreover, the phytotoxicity analysis signified the mineralization of toxic dye, Eriochrome Black T into low toxic products. Hence, this study offers a directed streamline for textile industries, encouraging bio-economic prospectives.

1. Introduction

Azo dyes are comprised of single or more azo linkages with aromatic groups and are categorized into distinct classes such as direct, mordant, acidic, basic, reactive, solvent and disperse dyes. They are widely applicable in diverse industrial sectors such as cosmetics, textile, paper and food (Pandey et al., 2007; Ramalingam and Devi, 2017). Azo dyes are inert, stable at high temperature, light conditions and at distinct pH ranges; they are also multifarious with wide range of colours. Hence, azo dyes are commercially used in the textile industries (Ogola et al., 2009; Ramalingam and Devi, 2017). The disposal of the effluents containing azo dyes, into the environment is toxic to marine organisms. For instance, the textile dyes can impede the solubility of oxygen in water and their intermediates dwell as the rootcause of mutagenicity and carcinogenicity in humans (Miranda et al., 2013). These toxic dyes can be eradicated and removed from effluent waste by both physical and chemical approaches such as oxidation, coagulation and adsorption (Crini, 2006). However, these treatments are expensive, not effectual for colour removal. In addition, these methods can also cause secondary hazards and pollutions because of the exorbitant chemical utility (Tamboli et al., 2010). Comparing to the former, the biological methods are highly promising as they are eco-friendly, cheap with low sludge. The current microbial studies on dye decolorization are majorly focussed on fungi and bacteria. Due to the high active and adaptable traits, bacteria are exclusively used in comparison to the fungus (Qu et al., 2010). Despite the fact that, the application of bacteria for dye treatment has attracted extensive attention, the reports on the recalcitrant dye biodegradation by actinobacterial peroxidases, are still limited (Roberts et al., 2011; Chen et al., 2015; Casciello et al., 2017). Therefore, it is requisite to exploit more actinobacteria, which has aptitude to degrade recalcitrant micro pollutants and carry out further researches on their characteristic traits.

To discern the potentiality of the enzyme to bind with substrate, researchers globally are targeted on incorporating the *in silico* methods such as biophysical modeling prior to ex situ or in situ bioremediation of toxic compounds for reducing the magnitude of time and cost. Biophysical modeling includes optimized molecular docking and dynamic simulations ligand diffusion to the active site of enzyme (Martínez et al., 2017). The docking studies are felicitous for explicit comprehensions of the significance and interaction between enzyme

* Corresponding author. School of Bio Sciences and Technology, Vellore Institute of Technology (VIT), Vellore, 632014, India.
E-mail addresses: saipreethi.p@vit.ac.in (P. Saipreethi), mrameshpathy@vit.ac.in (R. Manian).

https://doi.org/10.1016/j.bcab.2019.101127
Received 25 February 2019; Received in revised form 4 April 2019; Accepted 5 April 2019
Available online 10 April 2019
1878-8181/

and ligand (Sridhar and Chandra, 2014). As a supplementary, the prediction of amino acid residues interacting with dyes and enzyme is also achievable. Rahmanpur et al. have reported docking of wide panel of substrates to the TfuDyP structure, thereby suggesting a hydrogen bond involved conformation between the heme propionate side chain and hydroxyl group of the ligand (Rahmanpour et al., 2016). Guaiacol and Reactive Blue 5 were docked to Anabaena DyP active site, where a bound conformation was recounted on the heme cofactor distal face (Ogola et al., 2009).

The major intent of the present study was to validate a novel approach of integrating bioinformatics and actinobacterial peroxidase aided remediation for decolorization and transformation of azo dyes. It was targeted on the appliance of the active extracelluar peroxidase produced by the *Streptomyces coelicolor* SPR7, for decolorization of a six synthetic azo dyes such as Eriochrome Black T, Acid red 2, Metanil Yellow, Basic blue 9, Orange G and Diazin green. *In silico* investigation viz. Computational docking and analysis of binding site residues were executed to determine the interaction between the dyes and oxidoreductive enzyme like peroxidase, which is a promising tool for dye transformation and in addition, the amino acid residues present in binding site of the peroxidase were explored. Followed by this, the experimental degradation was carried out for the dye, Eriochrome black T (target dye with highest dock score) by purified peroxidase. The docking scores were highly correlating with the *in vitro* investigation viz. decolorization percentage. Peroxidase mediated biodegradation and biotransformation of Eriochrome black T was further confirmed by UV-vis spectroscopy (UV–vis), High Performance Liquid Chromatography (HPLC), Fourier Transform Infrared Spectroscopy (FTIR) and Gas Chromatography-Mass Spectroscopy (GC–MS). Hence, a cutting-edge and inexpensive *in silico* assisted *in vitro* methodology was validated for peroxidase aided treatment of Eriochrome black T, which is an applicable initiatory screening of the enzymatic dye transformations and thus, can be further recruited in industrial scale treatment of noxious textile dyes.

2. Materials and methods

2.1. Chemicals and textile dyes

All the azo dyes were purchased from HiMedia, India. The chemical structure and other dye attributes were presented in Table 1. The chemicals and dyes used in this study were of Analytical grade.

2.2. Isolation and identification of actinobacteria

The microbial source (marine sediments) used for isolation of actinobacterial strains was collected from Jaladi mangroves (13°39′41″N, 74°42′16″E) located in Karnataka, India. Actinobacterial strains were isolated using Starch Casein Agar (SCA) and Actinomycetes Isolation Agar (AIA) media and International *Streptomyces* Project 2 (ISP-2) medium (Ambavane et al., 2014; Kumar et al., 2014; Elbendary et al., 2018). Extraction and purification of genomic DNA was executed using CTAB as previously described (Kei et al., 2017). The amplification of genomic DNA was accomplished by Polymerase Chain Reaction (PCR). The PCR conditions and primers were according to previous protocols (Kumar et al., 2018). The sequences were analyzed through the MEGA 4.0. DNA Sequence of the isolate, was deposited in NCBI (GenBank accession no. **MH712067).**

2.3. Determination of enzyme activity and estimation of total protein

UV/Visible spectrophotometrically assay for peroxidase was performed at 30 °C by following the protocols proposed by Liu et al. with minor modifications. Peroxidase activity was monitored in a reaction volume of 2 mL using ABTS substrate as follows: the assay reaction system contained 0.1 mM H_2O_2, 0.5 mM ABTS, 100 mM sodium phosphate buffer (pH 6) and peroxidase. The substrate oxidation was measured at 420 nm (ε = 36,000 M-1 cm-1) and spectral changes were monitored spectrophotometrically (Evolution 300UV-VIS spectrophotometer, Thermo Scientific). The assay was executed in triplicates and the reaction mixture, devoid of the peroxidase was considered as the control (Liu et al., 2017). The crude supernatant obtained by centrifugation of the culture broth was recruited for total protein analysis by standard Bradford assay (Bradford, 1976).

2.4. Bioinformatics tools in dye biotransformation

2.4.1. Preparation of the protein and ligands

The protein Data Bank (PDB), aided retrieval of peroxidase protein structure with accession code: 4GU7. The PubChem compound databases (https://pubchem.ncbi.nlm.nih.gov/), aided acquitance of three dimensional structure of all the azo dyes in SDF format and their conversion into PDB files was accomplished by Online SMILES convertor and structure file generator (Weininger, 1988).

2.4.2. Chemical characterization and computational docking of azo dyes

The six azo dyes were chemically characterized by Mcule bioinfomatics webserver aided by property calculator tool with their respective canonical smiles as the input data. The docking analysis were performed by Autodock software Version 4.2, to determine the docking score and spot out the best docking poses of interactions between azo dyes and peroxidase in the docked ligand-enzyme complexes.

2.5. Comparative analysis between docking scores and degradation

The docking analysis of the six dyes with peroxidase was exhibited by comparing their dock scores with decolorization percentage obtained with *in vitro* studies. In addition, for confirming the dye degradation, analysis by HPLC, FTIR and GC–MS were also performed concomitantly for the analysis of the lower molecular products formed post to dye mineralization.

2.6. Purification of peroxidases

The purification of peroxidase was performed as described previously with slight modifications (Moubasher et al., 2017). The culture filtrate concentrated by ultrafiltration process in centrifugal microconcentrators with 10 KDa cut-off membranes (Amicon Inc., Beverly, MA, USA) was purified on Sephadex G-100 column (2 × 40 cm) by gel-permeation chromatography at room temperature after the column equilibration with100 mM potassium phosphate buffer (pH 7.0). The concentrated peroxidase solution was loaded on to the purification column and elution was performed with 100 mM potassium phosphate buffer (pH 7.0) at a flow rate of 0.5 ml/min. Distinct fractions (2 ml) were collected and their protein content was monitored at 280 nm. The kinetic activity of peroxidase was estimated only in fractions with higher protein content. The positive fractions displaying maximum peroxidase activity were pooled for storage at 4 °C and used for further appraisals.

2.7. Analytical gel electrophoresis

2.7.1. SDS-PAGE

The molecular weight and purity of the enzyme were estimated by SDS-PAGE (5% stacking and 10% separating gel) and the protein bands were visualized by silver nitrate staining (Karakus et al., 2018).

2.7.2. Zymogram analysis and activity staining

SDS-PAGE was performed under non-denaturing conditions and activity staining of peroxidase was visualized on 10% polyacrylamide gel at 50 V with minor modification as described by Achar et al., (2014). The protein mixed with sample buffer was loaded without any boiling. Post to electrophoresis, the gel was rinsed in water and

Table 1
Overture of Structure and characteristic features azo dyes used.

Dyes	Structure	Features	λmax
Eriochrome Black T	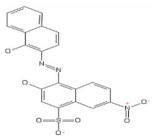	Mordant Black 11, Solochrome Black T, Hispacrom Black T, Magracrom Black A $C_{20}H_{12}N_3NaO_7S$ M.W: 415.38 g/mol CAS 1787-61-7	220 nm
Acid Red 2	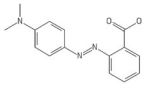	Methyl Red, O-methyl red, C.I. Acid Red 2, Cerven methylova $C_{15}H_{15}N_30_2$ M.W: 269.304 g/mol CAS 493-52-7	410 nm
Metanil Yellow	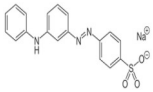	Monoazo, Amacid Yellow M, Acid yellow36,Acid Metanil Yellow $C_{18}H_{14}N_3NaO_3S$ M.W: 375.378 g/mol CAS 587-98-4	450 nm
Basic blue 9	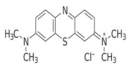	Swiss Blue, Methyl thioninium chloride, Methylene Blue, Urolene Blue $C_{16}H_{18}ClN_3S$ M.W: 319.851 g/mol CAS 61-73-4	670 nm
Orange G	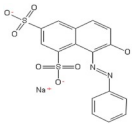	Wool Orange 2G, C.I. Food Orange 4, Acid Orange 10, C.I. Orange G $C_{16}H_{10}N_2Na_2O_7S_2$ M.W: 383.39 g/mol CAS 1936-15-8	476 nm
Diazin Green	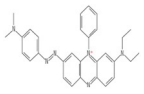	Janus Green V, Union Green B, Janus Green B. $C_{30}H_{31}ClN_6$ M.W:511.07 g/mol CAS 2869-83-2	λ1 = 395 nm; λ2 = 660 nm.

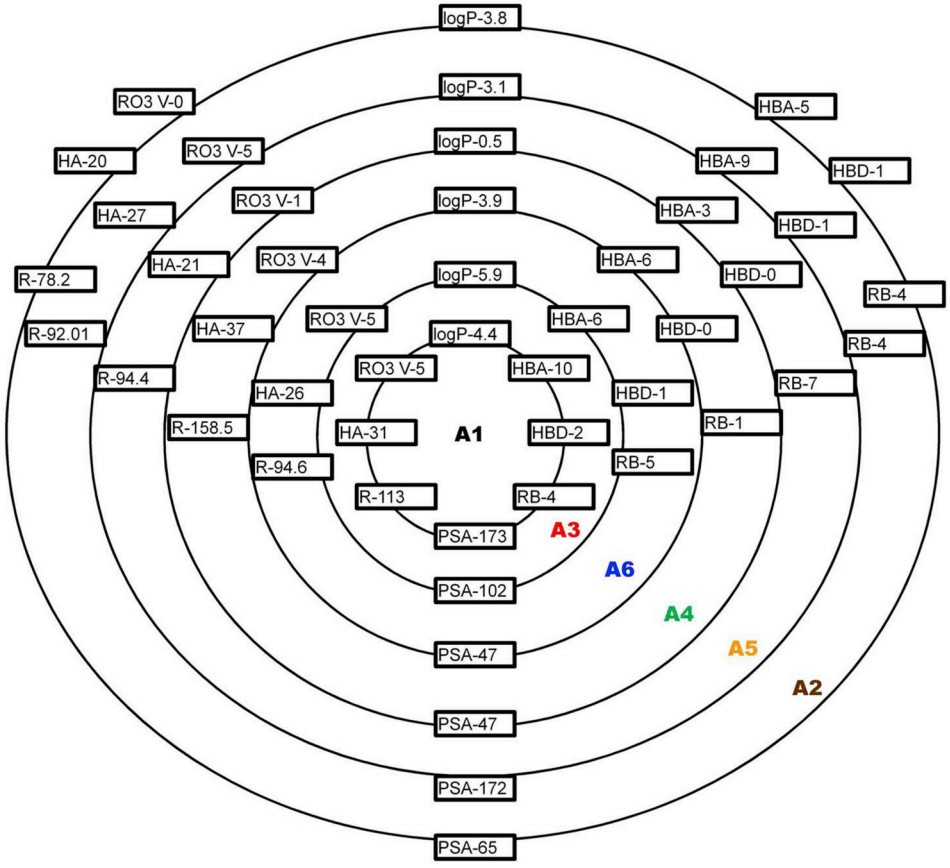

Fig. 1. Prediction of chemical properties of the six azo dyes, aligned based on their respective docking score. logP: log_{10} (partition coefficient); HBA: Hydrogen Bond Acceptors; Hydrogen Bond Donors; Rotatable Bonds; PSA: Polar Surface Area; R: Refractivity; HA: Heavy Atoms; Ro_3 violations: Rule of Three-criteria for chemical compounds.

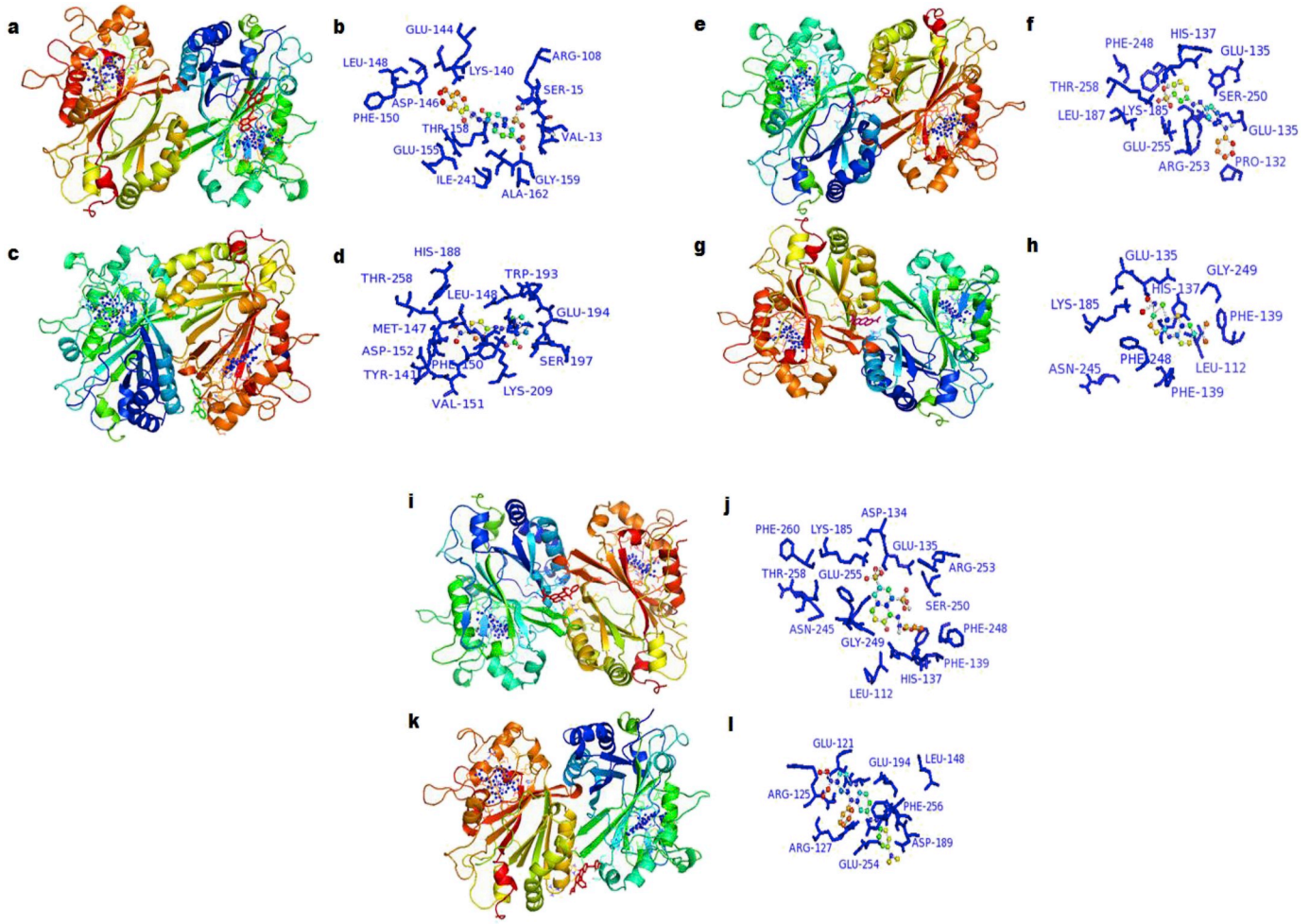

Fig. 2. Docked biomolecular complex of peroxidase *Streptomyces coelicolor* strain SPR7 peroxidase with various azo dyes and amino acid residues involved in the intermolecular interactions. a) & b) Eriochrome Black T; c) & d) Acid Red 2; e) & f) Metanil Yellow; g) & h) Basic Blue 9; i) & j) Orange G; k) & l) Diazin Green. (For interpretation of the references to color in this figure legend, the reader is referred to the Web version of this article.)

subjected to incubation in 10 ml of sodium phosphate buffer (pH-6) comprising of 1% Triton X-100 for 1 h. In order to remove Triton X-100, the gel was washed with distilled water and incubated for 10 min in 0.1 M phosphate buffer system (pH 6) containing: H_2O_2 (5%) and 1 mM ABTS as the chromogenic substrate.

2.8. Analysis of dye decolorization and degradation

Eriochrome Black T, a complexometric azo dye was selected for decolorization and remediation analysis by spectral and chromatographic techniques like UV–vis spectroscopy, HPLC, FTIR and GC–MS. The decolorization percentage was estimated spectrophotometrically (Evolution 300UV-VIS spectrophotometer, Thermo Scientific) for the dye sample degraded by peroxidase. The decolorization assay was performed by following modified protocol of Gomare and co-workers. The total reaction system consisted of 15 ml: 1 ml dye (100 ppm), 0.15 ml H_2O_2 (10 mM), 12.85 ml of 100 mM sodium phosphate buffer (pH 6) and purified peroxidase (3.5U/ml). The assay control contained all the constituents except the enzyme and decolorization was monitored at λmax of 220 nm. The experiments were carried out in triplicates. The degraded dye products were analyzed by HPLC, FTIR and GC-MS by extracting with ethyl acetate in equal volume. After extraction the samples were allowed to dry in rotary evaporator and the resulting residue was dissolved in analytical grade methanol (Gomare et al., 2008).

The HPLC (Shimadzu LC 40102010 system with dual absorbance detector) was performed on symmetrical C18 column (4.6 × 250 mm) using methanol as the mobile phase at 220 nm for 15 min at 1.0 mL min−1 of flow rate.

FTIR was performed in mid IR-region of 400–4000 cm−1 on PerkinElmer (spectrum RX I) with a scan speed of 16. The samples were analyzed for functional groups, by blending with KBr in the proportion (5: 95).

For GC–MS analysis of degraded dye intermediates, the 45XGC-44 gas chromatography (GC) coupled with Scion MS-40 mass spectroscopy (Bruker) was used and the Carrier gas (Helium) was availed for 26 min with 70 eV ionization voltage at a flow rate of 1.0 ml min−1. The analysis was accomplished using DB-WAX column (0.25–30 mm) with 80 °C as the initial temperature in oven for 2min and incremented up to 250 °C (10 °C min−1) and in addition, the NIST library was used for metabolite analysis.

2.9. Phytotoxicity analysis

The exposure of agricultural crops to noxious textile dyes and effluents can be a major cause of their undesirable physiological distortions such as photoperiodism, vernalization and photosynthesis etc. Therefore, determination of the toxicity attributes in these major crops is highly mandate. The phytotoxicity analysis was performed for treated and untreated dye samples (Tan et al., 2013). The ethyl acetate extract of lower breakdown products were dissolved in sterile distilled water after drying with rotary evaporator. The dicot crop, *Vigna radiata* (ten

Table 2
Assessment of correlation between *in silico* and *in vivo* analysis.

Dye	Ligand	Dock score (KJ/mol)	No. of Intermolecular hydrogen bonds	Residues with hydrophobic interactions	Decolorization (%)	
					6 h	12 h
Eriochrome Black T	A1	-7.2	8 (Val13*,Ser15*,Gly159*)	Glu144,Lys140,Arg108,Ala162,Ile241,Glu155, Thr158,Asp146,Phe150,Leu148.	68.3	94.21
Acid Red 2	A2	-4.67	1 (Lys209*)	His188, Leu148,Trp193,Glu194,Ser197,Val151,Phe150,Tyr141,Asp152,Met147,Thr258.		
Metanil Yellow	A3	-7.03	4 (Lys185*,Glu135*)	His137,Ser250, Pro132,Arg253,Glu255,Leu187, Thr258,Phe248		
Basic blue 9	A4	-6.5	1(His137*)	Glu135,Gly249,Phe139,Leu112,Phe139,Phe248,Asn245, Lys185.		
Orange G	A5	-6.0	4 (Lys185*, Glu135*, His137*)	Asp134,Arg253, Ser250, Phe248, Phe139,Leu112,Gly249,Asn245,Glu255,Thr258, Phe260.		
Diazin Green	A6	-6.87	–	Glu121, Glu194, Leu148,Phe256, Asp189,Glu254, Arg127, Arg125		

seeds) were subjected to treatment with extract of the dye, Eriochrome Black T (100 ppm) or its catabolic products. The assays run concomitantly with distilled water, dwelled as the control. The germination percentage (%), length of the radical and plumule were observed after 5 days. The germination percentage was determined by the equation as follows:

$$\text{Germination}(\%) = \frac{\text{Number of seed germinated}}{\text{Number of seeds sowed}} \text{X}100 \quad (1)$$

2.10. Statistical analysis

The data were statistically analyzed by one-way analysis of variance (ANOVA) using GraphPad Prism 7.03 software for significance at $P \leq 0.05$ and all the experiments were run in triplicate.

3. Result and discussion

3.1. Isolation and identification of peroxidase producing actinobacteria

A total of 20 isolates of actinomycetes were derived from the soil samples of Jaladi mangroves and amidst which the isolate, VITJM7 dwelled as the best producer of peroxidase and hence, this strain was selected for further analysis. The16S rDNA sequence based homological study of the VITJM7, revealed the 99% similarity of the isolate with *Streptomyces coelicolor* (GenBank accession no. AB588124.1) and hence, the isolate assigned as *S. coelicolor* strain SPR7. A broad battery of commercial azo dyes associated with textile uses can be mineralized by multifarious *Streptomyces* taxa. In the manner that, the isolate *S. coelicolor* strain SPR7, manifested its potentialistic role in degradation of Eriochrome Black T. In a similar vein, the isolate, *Streptomyces* DJP15 displayed a bioremediatory role on the textile dye namely, azo blue (Pillai, 2017). In addition, *Streptomyces krainskii* SUK -5 exhibited the biotransformation of the azo dye, Reactive blue-59 through the catalytic role of lignin peroxidase (Mane et al., 2008). However, adding on to the actinomycetes, the role of bacteria (*Bacillus subtilis, Aeromonas hydrophila* MTCC 1739 and *Lysinibacillus sphaericus* MTCC 9523), fungi (*Aspergillus bombycis)* and mushroom (*Lentinula edodes*) in azo dye mineralization has also been well established (Boer et al., 2004; Kumar et al., 2015; Khan and Fulekar, 2017; Srinivasan and Sadasivam, 2018).

3.2. Peroxidase activity and total protein yield

S. coelicolor strain SPR7 was cultivated in starch caesin liquid medium without the incorporation of the additional inducers. The characteristic growth of the isolate lasted up to 56 h, after which an access into the stationary phase was observed, enduring up to 98 h. Over and above, a higher production of the enzyme (specific activity 0.017U/mg and Peroxidase activity 360 U/L) with a total protein yield of 20,779 μg/L was displayed in stationary phase, although a preliminary productivity of peroxidase was manifested in exponential phase. Some previous investigations recorded similar results. However, the peroxidase generation displayed by *S. coelicolor* strain SPR7 was significantly higher in comparison to that of previous reports. To specify, *Streptomyces* strain EC22 was competent to produce around 270U/L of an extracellular peroxidase (Mercer et al., 1996) and *Streptomyces* sp. K37 evinced peroxidase activity of 350U/L (El-Dein et al., 2014). The major reason for the significant difference in the catalytic activity of peroxidase observed with *S. coelicolor* strain SPR7 in comparison with the documented studies is incomprehensible howbeit; it is an incentive for the upcoming investigations. Nevertheless, the peroxidase activity revealed by *S. coelicolor* strain SPR7 is highly consistent with the catalytic activity against ABTS.

Table 3
Purification of peroxidase from *S. coelicolor* SPR7 fermentation broth.

Sample	Volume (ml)	Total protein (μg/ml)	Activity (U/ml)	Total activity (U/ml)	Specific activity (U/mg)	Purification Fold	Yield %
Crude broth	500	10,388	0.36	180	0.0173	1	100
Filtration-Concentration	82	898.32	2.1	172.2	0.194	11.4	95.5
Sephadex G-100	18	70.128	3.5	63	0.893	51.6	35

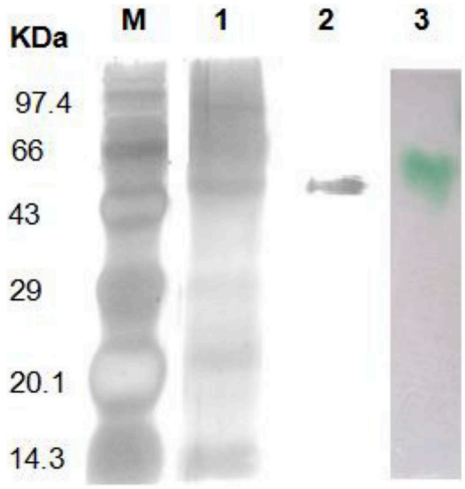

Fig. 3. Electrophoretic analysis of peroxidase from *Streptomyces* culture broth. SDS-PAGE analysis of (1) Crude soluble enzyme and (2) Purified enzyme obtained by Sephadex G-100 chromatographic column.(3) peroxidase activity staining by zymogram analysis with ABTS as the substrate. M: marker proteins of known molecular mass.

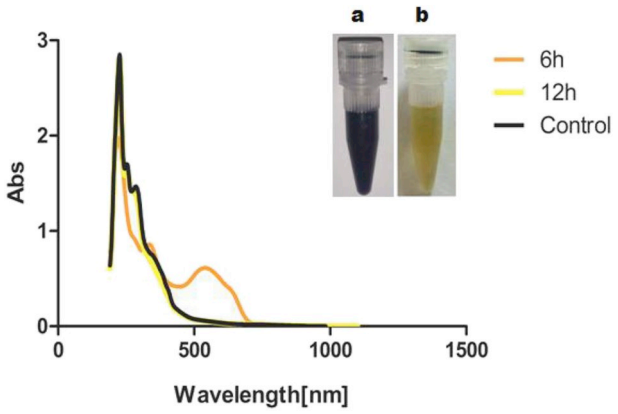

Fig. 4. UV- VIS spectral profiles of Eriochrome Black T biodegradation. Spectral scans depict (100 ppm) biodegradation by 3.5 U/mL of *Streptomyces coelicolor* strain SPR7 purified peroxidase at various incubation periods, pH 6; Temperature 37 °C.

3.3. Chemical properties and computational docking of azo dyes

The distinct chemical properties and specifications of the six azo dyes were elucidated based on their molecular docking scores (Fig. 1). Autodock software was employed for computational docking and analysis of ligand-protein interactions of all the six azo dyes *viz*. Eriochrome Black T, Acid red 2, Metanil Yellow, Basic blue 9, Orange G and Diazin green with peroxidase of *S. coelicolor* strain SPR7 (Fig. 2a-l). The amino acid residues of binding pocket, docking scores and binding mode were scrutinized. The binding energy was used as an essential criteria for the selection of the target dye and out of all the six dyes recruited in the study, Eriochrome Black T displayed the highest

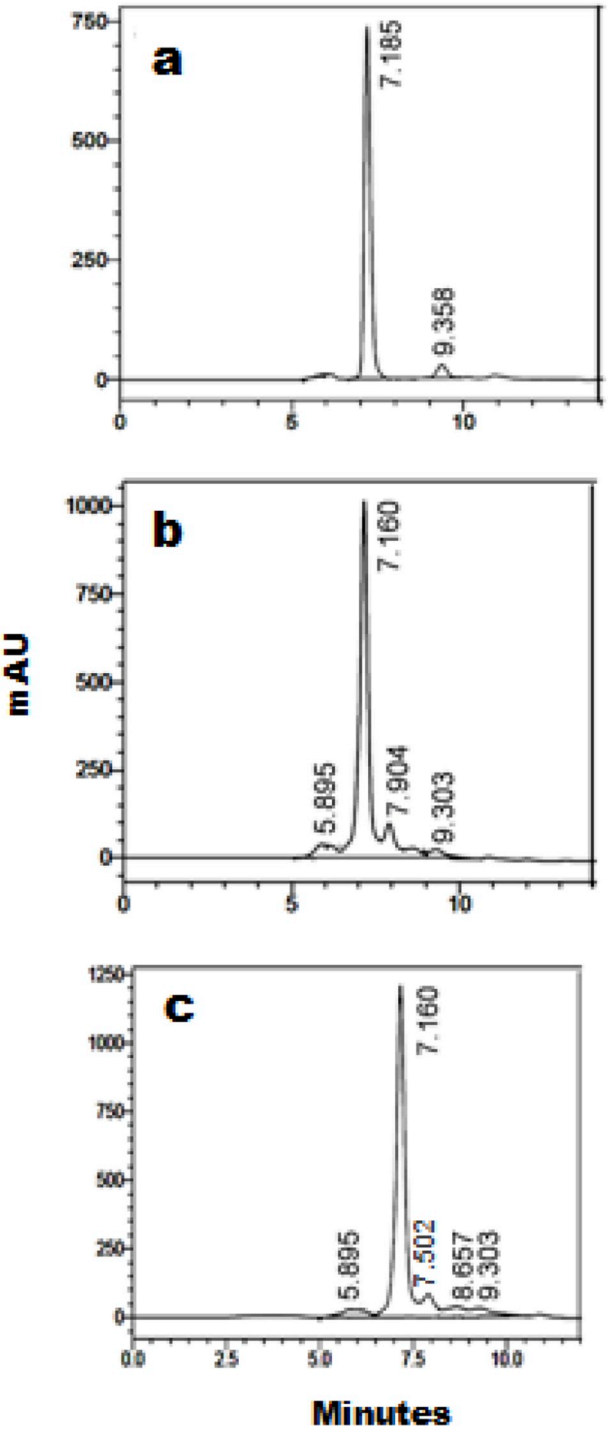

Fig. 5. HPLC elution profile of Eriochrome Black T biotransformation by purified peroxidase of *Streptomyces coelicolor* strain SPR7 at distinct incubation periods (a: Eriochrome Black T control, b: 6 h, c: 12 h).

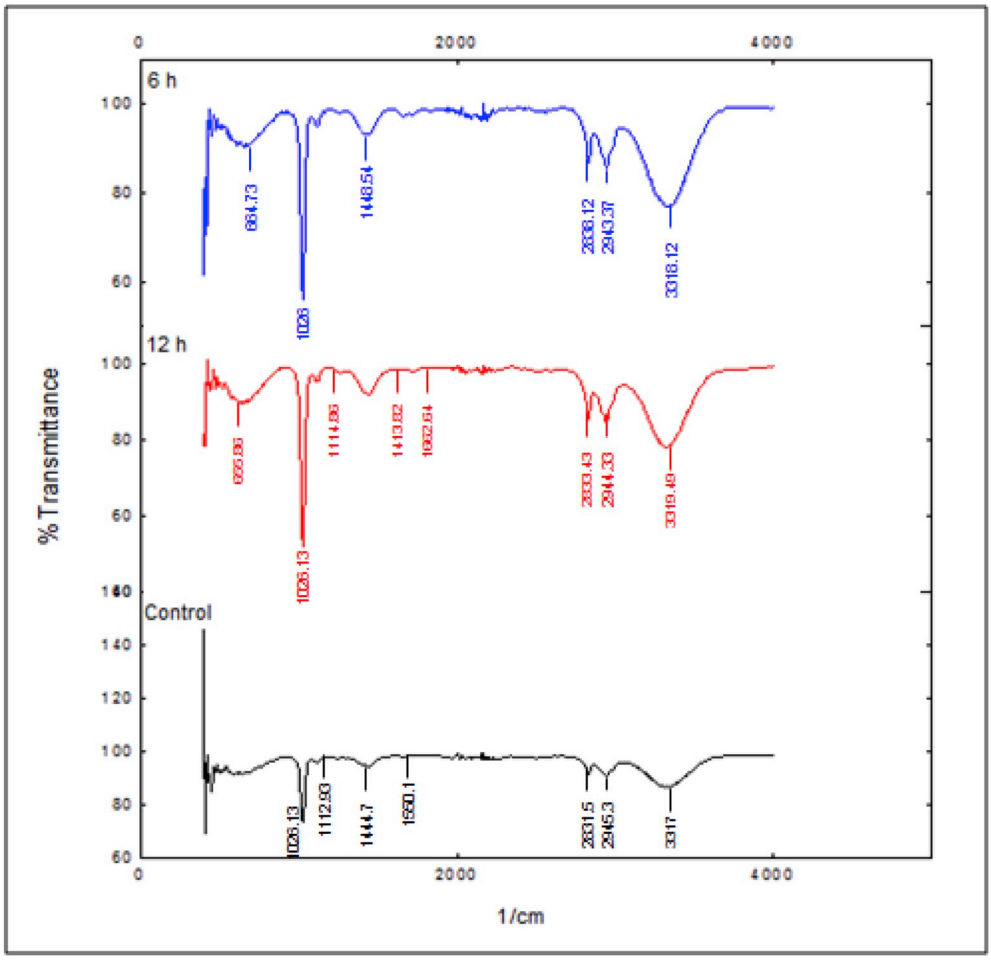

Fig. 6. FT-IR spectra of Eriochrome Black T biotransformation by *Streptomyces coelicolor* strain SPR7 peroxidase and the untreated dye control.

negative binding energy (-7.2 kJ/mol) with peroxidase. Contradicting with the above result, methyl red manifested a least negative binding energy of -4.67 kJ/mol. The descending order of the binding affinity of all the azo dyes with receptor enzyme is given as follows: A1 > A3 > A6 > A4 > A5 > A2, where A1 epitomizes the strongest interaction amidst the six ligands and supplementary to these factors, the hydrogen bond plays a vital role in the stabilization of ligand-receptor interaction (Table 2). The *in silico* appraisals *viz.* active site residues and molecular docking studies with textile azo dyes have been demonstrated previously (Hadibarata et al., 2013).

3.4. In silico and in vitro-correlation

The docking score exhibits an associated relationship with decolorization rate and henceforth the former shows a direct proportionality to the latter phenomenon (kumar et al., 2016). Hence, lowest binding energy needed by *S. coelicolor* POX displays its higher interaction with Eriochrome Black T. Wherefore, citing a higher rate of corroboration with the *in-vitro* degradation of dyes. The appraisal of relationship between docking and peroxidase aided decolorization of the Eriochrome Black T revealed a higher rate of association. Table 2, accentuates the comparative analysis of *in silico* and *in vitro* results for the dye, Eriochrome Black T.

3.5. Purification of peroxidase

The purification of the extracellular oxidoreductive peroxidase was accomplished using the gel-filtration chromatography. The enzyme was purified 51.6 folds with specific activity 0.893 U/mg signifying the higher scale of the enzyme purity. The purification steps have been elucidated in Table 3. The proficiency of the purification method was validated through 10% SDS PAGE, which evinced only a single protein band of 45 KDa with peroxidase activity by zymogram staining (Fig. 3). The molecular weights of other *Streptomyces* sp. have been recounted earlier reports ranging from 17 to 60 KDa (Ramachandra et al., 1988; Fodil et al. 2011, 2012).

3.6. Degradation analysis of dye metabolites formed by purified peroxidase

The efficacy of peroxidase generated by *S. coelicolor* strain SPR7 in biotransformation of the dye, Eriochrome Black T was scrutinized via changes in the peak intensity of absorbance by measuring the optical density at λmax of 220 nm at distinct time intervals of 6 and 12 h (Fig. 4). The spectral plot of dye control was characterized by an absorbance peak at 220 nm for blackish maroon colour, which relates to conjugated azo chromophore. With the former as the reference for conformation of dye mineralization, the degradative strategies were monitored for enzyme treated dye samples. Interestingly, a noteworthy absorbance reduction of the treated samples with the simultaneous increase in the incubation timeline was manifested, propounding the azo bond cleavage and degradation of dye associated chromophore contributing to the decolorization. It was perceived that the dye was mineralized 68.3 and 94.21% by purified peroxidase at the incubation timelines of 6, 12 h respectively (Table 2). The decolorization of the dyes is associated with the azo bond reduction coupled with the presence of anoxic environment by the oxidoreductive enzymes (Sarkar et al., 2017).

Oon et al., (2018), used a composite approach of up-flow

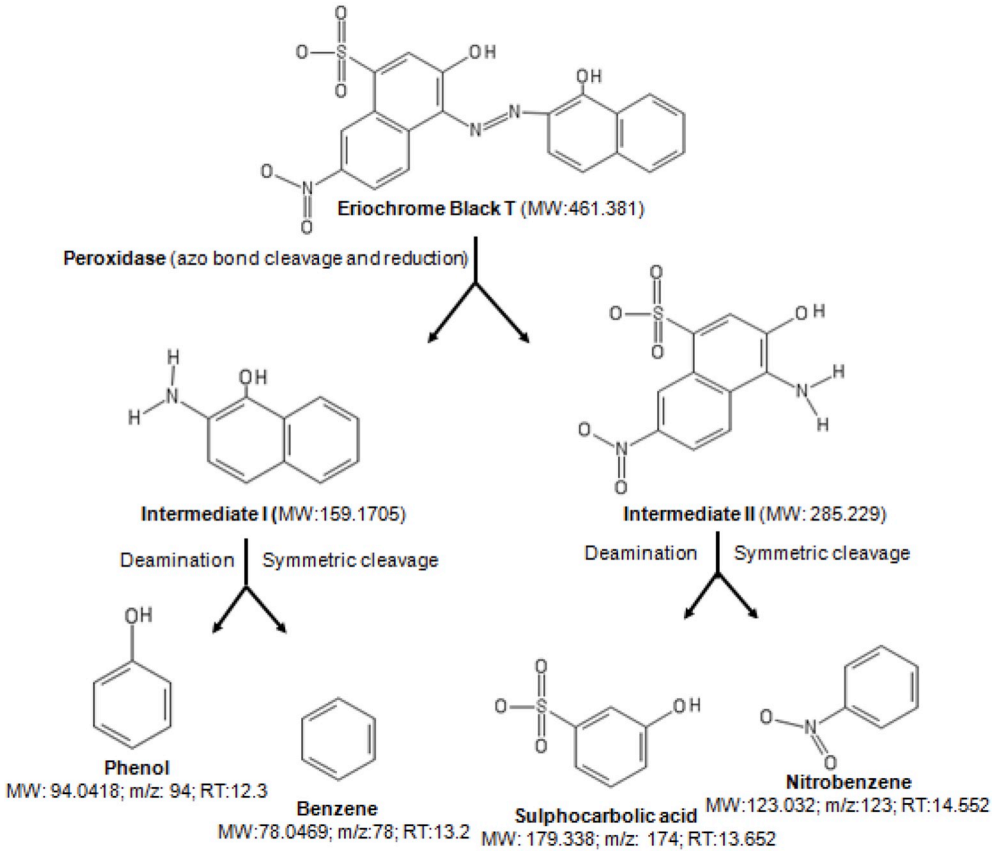

Fig. 7. Proposed pathway for symmetrical azo bond cleavage of Eriochrome Black T by peroxidase of *S. coelicolor* strain SPR7.

Table 4
Phytotoxicity analysis of Eriochrome Black T (100 ppm) and its degraded metabolites on *Vigna radiata*.

Parameters studied	Distilled water	Eriochrome Black T	Extracted metabolites	
			6 h	12 h
Germination (%)	60%	20%	40%	50%
Plumule (cm)	9.05 ± 0.05	7.5 ± 0.13	1.725 ± 0.175	1.86 ± 0.508
Radical (cm)	0.75 ± 0.2	0.3 ± 0.1	0.55 ± 0.05	1.08 ± 0.504

constructed wetland-microbial fuel cell cum biodegradation approach for Acid Red-18, accounting for 91% of dye transformation. Contrarily, Gomare and co-workers recorded a prolific role of lignin peroxidase for bioremediation of azo dyes such as Methyl Orange and Blue-2B (Gomare et al., 2008). Adding on to these findings, a typical strategy has been well established by Song et al., (2017), who recounted a significant role of lignin and manganese peroxidase in the degradation of textile azo dye, Acid Red B (98.15% within 6 h) by salt tolerant yeast, *Pichia occidentalis* G1. Hence, these findings reveal that the marine microbial systems are proficient peroxidase producers, intuited to transform the toxic azo dyes.

The HPLC appraisals of control dye samples evinced a major peak at retention time of 7.185 min and a minor peaks at 9.358 min, dwelling consistency to the retention time of native dye solution (Fig. 5a). After 6 h of decolorization by purified peroxidase, the peak intensity at retention time of 9.358 min descended and a generation of new peak was marked out at retention time of 5.895, 7.904 and 9.303 min signifying the degradation of the parental dye streams (Fig. 5b). Execution of the degradation process further until 12 h, resulted in the reduction in the peak intensity at 7.904 min with new peaks at 7.502 and 8.657 min, validating the biodegradation strategy of Eriochrome Black T by purified peroxidase of *S. coelicolor* strain SPR7 into low molecular weight metabolites (Fig. 5c). Gomare and co-workers stated that HPLC chromatogram of methyl orange mineralized by lignin peroxidase of *Brevibacillus laterosporus* displayed peaks at retention time of 1.816, 2.616 and 2.847 min, while the control samples showed peak at 1.698 min, propounding the breakdown of the dye into smaller products (Gomare et al., 2008).

FTIR associated mid-IR (400–4000 cm^{-1}) finger printing region exemplifies the distinct peaks of various overlapping and characteristic functional groups confined to the intact dye moiety. The dye control and transformed metabolites records the biomineralization of complex noxious dye into simpler products. The untreated control sample of Eriochrome Black T displays corresponding peaks in the categorical frequency region of the various functional groups (Fig. 6). Peak at 3317 cm − 1 for OH stretching, followed by the peak between 1500 cm − 1 and 1600 cm − 1 for −N═N- stretching of azo group (Balapure et al., 2015), 2945.3 and 2831.5 cm − 1 for symmetrical and asymmetrical C—H stretching, 1444.7 cm − 1 for C═C stretching in aromatic compounds, 1112.93 cm − 1 assigned to C—O stretching vibrations of acids, 1026.13 cm − 1 for C—O stretching in phenols.

The FTIR spectral profile of the enzyme treated dye for 6 h, displayed a sharp peak at 3318.2 cm − 1 for OH stretching, 2943.37 cm − 1 for symmetrical C—H stretching, 2838.12 cm − 1 for symmetrical and asymmetrical C—H stretching, 1448.54 cm − 1 for C═C stretching in aromatic metabolites, 1026 cm − 1for C—O stretching in phenols and formation of new peak at 664.73 cm − 1 conjugated with the characteristic C—H stretching, indicates the spectral changes emerged upon Eriochrome black T degradation. After 12 h of incubation timeline, the spectral plot showed up a peak at 3319.49 cm − 1 depicting the stretching of hydroxyl group, 2944.33 cm − 1 for symmetrical C—H stretching, 2833.43 cm − 1 for asymmetrical C—H stretching, 1662.64 cm − 1 for azo bond cleavage, 1413.82 cm − 1 for S═O stretching,

1114.86 cm − 1 assigned to C—O stretching vibrations of acids, 1026.13 cm − 1 for C—O stretching in phenols and 655.86 cm − 1 reveals stretching of C—H bonding. These results clearly support the peroxidase catalyzed dye breakdown and infrared spectral findings have also been proposed earlier for azo dyes like methyl orange (Gomare et al., 2008) and Acid Blue 113 (Shanmugam and Mahadevan, 2015).

GC–MS appraisal of the mineralized Eriochrome black T products, propounded the formation of simpler metabolites with lower molecular weight validating the transformation of Eriochrome black T by the enzyme. The pathways of Eriochrome black T by the peroxidase moiety were set forth on the basis of molecular weight (MW), mass to charge ratio (m/z) and retention time (RT) of products from GC–MS and NIST library analysis.

An overture of GC–MS peaks of the enzyme treated dye are illustrated (Table SM 1). The cleavage of the azo bond present in the dye, is accomplished by the catalytic reductive role of peroxidase consequently to form intermediates I & II. Upon execution of the degradative strategies, the intermediate I was subjected to symmetrical cleavage, followed by the deamination process to form the aromatics viz. benzene (MW: 78.0469; m/z: 78; RT: 13.2) and ultimately phenol (MW: 94.0418; m/z: 94; RT: 12.3). Interestingly the Intermediate II was set forward to form acidic product stream such as sulfocarbolic acid (MW: 179.338; m/z: 174; RT: 13.652) and nitrobenzene (MW: 123.032; m/z: 123; RT: 14.552). The chemical mechanism of peroxidase-mediated Eriochrome black T transformation pathway is propounded based upon the reaction chemistry between the dye and the enzyme (Fig. 7). Wide panel of investigations have recorded the results based on the azo dye bioremediations with the bacterial enzymes as the promising tool with the initial cleavage of azo bond to form distinctive aromatic amines that are converted further into simple aromatic compounds (Balapure et al., 2015; Srinivasan and Sadasivam, 2018). Hence, the analytical studies viz. UV-vis, FTIR, HPLC and GC-MS were highly supportive for the degradation of Eriochrome black T.

3.7. Phytotoxicity studies on Vigna Radiata

Seeds of *Vigna Radiata* (Mung bean) were selected to test their sensitivity towards Eriochrome black T and its degraded metabolites, the results were elucidated in Table 4. The germination percentage of seeds treated with Eriochrome black T (20%) was lower than those treated by distilled water as the control (60%) and its degraded metabolites 6 h (40%) and 12 h (50%). The statistical mean of radicle and plumule lengths were 0.75 ± 0.2 and 9.05 ± 0.05 cm, respectively for ten seeds using sterile distilled water.

Contrastingly, the length of root and shoot systems were drastically affected after treatment with Eriochrome Black T (100 ppm). However, the degraded compounds of Eriochrome black T, revealed a lower toxic profile on *V. radiata* as the radicle and plumule lengths were higher than the pure dye mixture i.e., 1.08 ± 0.504 and 1.86 ± 0.508 cm respectively after 12 h of incubation timeline (Table 4). Supporting these observations, demonstrations of non-phytotoxic attributes have been prophesized previously using biologically treated dye samples in comparison to the control streams on *V. Radiata* (Haq et al., 2018).

4. Conclusion

In the current study, purified peroxidase of *S. coelicolor* strain SPR7 was employed for the biotransformation of a synthetic textile azo dye, Eriochrome Black T, also known as Mordant Black 11. Although the isolate is not from textile arena, the efficacy of the isolate to produce noteworthy and active dye degrading peroxidase is propounded in the study. Hence, it is unerring to state that this enzyme can be a prominent and resourceful biocatalyst for textile –based and azo dye containing effluent treatment without any conglomeration of mediators. Interestingly, the docking studies were corroborative with the degradation analysis. Molecular docking could be an excellent tool in large-scale enzyme screening to choose the most potential decolorizer. Thus a coupled remediation scheme, contemplating theoretical computational strategies and subsequent microbial validation has been executed to constrict the time and outgoings needed for *in vitro* experimental analysis. Thereby, these results dwell to authenticate the pioneering role of bioinformatics for exposure of the promising biocatalyst channelizing the safe, economic and eco-friendly approach of toxic azo dyes.

GC-MS appraisal of peroxidase treated dye mixture, validated the mineralization of Eriochrome Black T, demonstrating the process of decolorization and degradation through the azo bond cleavage and deamination. Furthermore, the phytotoxicity analysis signified the reduced toxicity of degraded metabolites on *Vigna radiata*. Ultimately, these findings would be a proficient streamline for a systematic operation of textile effluent containing azo dyes for large scale industrial applications, wherefore exhibiting less toxicity on agriculturally important crops, retaining a sustainable green environment from these dyestuffs and pigments, comprising of recalcitrant compounds from organochloride to highly noxious heavy metals.

Conflicts of interest

The authors declare that they have no conflict of interest.

Acknowledgements

The authors gratefully acknowledge the management of Vellore Institute of Technology, Vellore for providing the seed money to support and encourage our research work. This research did not receive any grants from funding agencies in the public, commercial, or not-for-profit sectors.

Appendix A. Supplementary data

Supplementary data to this article can be found online at https://doi.org/10.1016/j.bcab.2019.101127.

References

Achar, R.R., Venkatesh, B.K., Sharanappa, P., Priya, B.S., Swamy, S.N., 2014. Evidence for peroxidase activity in *Caralluma umbellata*. Appl. Biochem. Biotechnol. 173, 1955–1962.

Ambavane, A., Tokdar, P., Parab, R., Sreekumar, E.S., Mahajan, G., Mishra, P.D., D'Souza, L., Ranadive, P., 2014. Caerulomycin A - an antifungal compound isolated from marine actinomycetes. Adv. Microbiol. 4, 567–578.

Balapure, K., Bhatt, N., Madamwar, D., 2015. Mineralization of reactive azo dyes present in simulated textile waste water using down flow microaerophilic fixed film bioreactor. Bioresour. Technol. 175, 1–7. https://doi.org/10.1016/j.biortech.2014.10.040.

Boer, C.G., Obici, L., Marques de Souza, C.G., Peralta, R.M., 2004. Decolorization of synthetic dyes by solid state cultures of *Lentinula* (Lentinus) *edodes* producing manganese peroxidase as the main ligninolytic enzyme. Bioresour. Technol. 94, 107–112.

Bradford, M.M., 1976. A rapid and sensitive method for the quantitation of microgram quantities of protein utilizing the principle of protein-dye binding. Anal. Biochem. 72, 248–254. https://doi.org/10.1016/0003-2697(76)90527-3.

Casciello, C., Tonin, F., Berini, F., Fasoli, E., Marinelli, F., Pollegioni, L., Rosini, E., 2017. A valuable peroxidase activity from the novel species *Nonomuraea gerenzanensis* growing on alkali lignin. Biotechnol. Rep. 13, 49–57. https://doi.org/10.1016/j.btre.2016.12.005.

Chen, C., Shrestha, R., Jia, K., Gao, P.F., Geisbrecht, B.V., Bossmann, S.H., Shi, J., Li, P., 2015. Characterization of dye-decolorizing peroxidase (DyP) from *Thermomonospora curvata* reveals unique catalytic properties of A-type DyPs. J. Biol. Chem. 290, 23447–23463.

Crini, G., 2006. Non-conventional low-cost adsorbents for dye removal: a review. Bioresour. Technol. 97, 1061–1085. https://doi.org/10.1016/j.biortech.2005.05.001.

Elbendary, A.A., Hessain, A.M., El-Hariri, M.D., Seida, A.A., Moussa, I.M., Mubarak, A.S., Kabli, S.A., Hemeg, H.A., El Jakee, J.K., 2018. Isolation of antimicrobial producing actinobacteria from soil samples. Saudi J. Biol. Sci. 25, 44–46. https://doi.org/10.1016/j.sjbs.2017.05.003.

El-Dein, M.M.N., Shereif, A.E.A., Mansour, F.A., Abou-Dobara, M.I., Ball, A.S., 2014. Optimization of xylanase and peroxidase production from *Streptomyces* sp. K37. J. BioSci. Biotech 3, 29–42.

Fodil, D., Badis, A., Jaouadi, B., Zaraî, N., Ferradji, F.Z., Boutoumi, H., 2011. Purification

and characterization of two extracellular peroxidases from *Streptomyces* sp. strain AM2, a decolorizing actinomycetes responsible for the biodegradation of natural humic acids. Int. Biodeterior. Biodegrad. 65, 470–478. https://doi.org/10.1016/j.ibiod.2011.01.009.

Fodil, D., Jaouadi, B., Badis, A., Zaraî, N., Ferradji, F.Z., Bejar, S., Boutoumi, H., 2012. A thermostable humic acid peroxidase from *Streptomyces* sp. strain AH4: purification and biochemical characterization. Bioresour. Technol. 111, 383–390. https://doi.org/10.1o16/j.biortech.2012.01.153.

Gomare, S.S., Jadhav, J.P., Govindwar, S.P., 2008. Degradation of sulfonated azo dyes by the purified lignin peroxidase from *Brevibacillus laterosporus* MTCC 2298. Biotechnol. Bioproc. Eng. 13, 136–143.

Hadibarata, T., Adnan, L.A., Yusoff, A.R.M., Yuniarto, A., Rubiyatno, Zubir, M.M.F.A., Khudhair, A.B., Teh, Z.C., Naser, M.A., 2013. Microbial decolorization of an azo dye reactive black 5 using white-rot fungus *Pleurotus eryngii* F032. Water Air Soil Pollut. 224, 1595.

Haq, I., Raj, A., Markandeya, 2018. Biodegradation of Azure-B dye by *Serratia liquefaciens* and its validation by phytotoxicity, genotoxicity and cytotoxicity studies. Chemosphere 196, 58–68. https://doi.org/10.1016/j.chemosphere.2017.12.153.

Karakus, Y.Y., Acemi, A., Işık, S., Duman, Y., 2018. Purification of peroxidase from *Amsonia orientalis* by three-phase partitioning and its biochemical characterization. Separ. Sci. Technol. 53, 756.

Kei, F., Sawamura, T., Niwa, T., Deyama, T., Nomura, S.M., Taguchi, H., Doi, N., 2017. In vitro transcription–translation using bacterial genome as a template to reconstitute intracellular profile. Nucleic Acids Res. 45, 11449–11458.

Khan, R., Fulekar, M.H., 2017. Mineralization of a sulfonated textile dye Reactive Red 31 from simulated wastewater using pellets of *Aspergillus bombycis*. Bioresour. Bioprocess. 4, 23.

Kumar, A., Chopra, J., Singh, S.K., Khan, A., Singh, R.N., 2015. Biodegradation of azo dyes by *Bacillus subtilis* 'RA29'. 7. Der Pharmacia Lettre, pp. 234–238.

Kumar, J.G.S.P., Gomathi, A., Gothandam, K.M., Vasconcelos, V., 2018. Bioactivity assessment of Indian origin—Mangrove actinobacteria against *Candida albicans*. Mar. Drugs 16, 60.

Kumar, S.P., Duraipandiyan, V., Ignacimuthu, S., 2014. Isolation, screening and partial purification of antimicrobial antibiotics from soil *Streptomyces* sp. SCA 7. Kaohsiung J. Med. Sci. 30, 435–446.

Kumar, S.S., Shantkriti, S., Muruganandham, T., Murugesh, E., Rane, N., Govindwar, S.P., 2016. Bioinfomatics aided microbial approach for bioremediation of wastewater containing textile dyes. Ecol. Inf. 31, 112–121. https://doi.org/10.1016/j.ecoinf.2015.12.001.

Liu, C., Zheng, K., Xu, Y., Stephen, L.T., Wang, J., Zhao, H., Yue, H., 2017. Expression and characterization of soybean seed coat peroxidase in *Escherichia coli* BL21 (DE3). Prep. Biochem. Biotechnol. 47, 768–775.

Mane, U., Gurav, P., Deshmukh, A., Govindwar, S., 2008. Degradation of textile dye reactive Navy blue RX (Reactive blue-59) by an isolated actinomycete *Streptomyces krainskii* SUK-5. Mal. J. Microbiol. 4, 1–5.

Martínez, A.T., Ruiz-Dueñas, F.J., Camarero, S., Serrano, A., Linde, D., Lund, H., Vind, J., Tovborg, M., Herold-Majumdar, O.M., Hofrichter, M., Liers, C., Ullrich, R., Scheibner, K., Sannia, G., Piscitelli, A., Pezzella, C., Sener, M.E., Kılıç, S., van Berkel, W.J.H., Guallar, V., Lucas, M.F., Zuhse, R., Ludwig, R., Hollmann, F., Fernández-Fueyo, E., Record, E., Faulds, C.B., Tortajada, M., Winckelmann, I., Rasmussen, J.A., Gelo-Pujic, M., Gutiérrez, A., del Río, J.C., Rencoret, J., Alcalde, M., 2017. Oxidoreductases on their way to industrial biotransformations. Biotechnol. Adv. 35, 815–831. https://doi.org/10.1016/j.biotechadv.2017.06.003.

Mercer, D.K., Iqbal, M., Miller, P.G.G., McCarthy, A.J., 1996. Screening actinomycetes for extracellular peroxidase activity. Appl. Environ. Microbiol. 62, 2186–2190.

Miranda, Rde C., Gomes, Ede B., Pereira Jr, N., MarinMorales, M.A., Machado, K.M., Gusmao, N.B., 2013. Biotreatment of textile effluent in static bioreactor by *Curvularia lunata* URM 6179 and *Phanerochaete chrysosporium* URM 6181. Bioresour. Technol. 142, 361–367. https://doi.org/10.1016/j.biortech.2013.05.066.

Moubasher, H., Mostafa, F.A., Wahsh, S., Haroun, O., 2017. Purification and characterization of lignin peroxidase isozymes from *Humicola grisea* (Traaen) and its application in bioremediation of textile dyes. Egypt. J. Bot. 57, 335–343.

Ogola, H.J.O., Kamiike, T., Hashimoto, N., Ashida, H., Ishikawa, T., Shibata, H., Sawa, Y., 2009. Molecular characterization of a novel peroxidase from the cyanobacterium *Anabaena* sp. strain PCC 7120. Appl. Environ. Microbiol. 75, 7509–7518.

Oon, Y.L., Ong, S.A., Ho, L.N., Wong, Y.S., Dahalan, F.A., Oon, Y.S., Lehl, H.K., Thung, W.E., Nordin, N., 2018. Up-flow constructed wetland-microbial fuel cell for azo dye, saline and nitrate remediation and bioelectricity generation: from waste to energy approach. Bioresour. Technol. 266, 97–108. https://doi.org/10.1016/j.biortech.2018.06.035.

Pandey, A., Singh, P., Iyengar, L., 2007. Bacterial decolorization and degradation of azo dyes. Int. Biodeterior. Biodegrad. 59, 73–84. https://doi.org/10.1016/j.ibiod.200608.006.

Pillai, H.P.J.S., 2017. Optimization of process conditions for effective degradation of azo blue dye by *Streptomyces* DJP15. J. Pure Appl. Microbiol. 11, 1757–1765. https://doi.org/10.22207/JPAM.11.4.14.

Qu, Y., Shi, S., Ma, F., Yan, B., 2010. Decolorization of reactive dark blue K-R by the synergism of fungus and bacterium using response surface methodology. Bioresour. Technol. 101, 8016–8023. https://doi.org/10.1016/j.biortech.2010.05.025.

Rahmanpour, R., Rea, D., Jamshidi, S., Fülop, V., Bugg, T.D., 2016. Structure of *Thermobifida fusca* DyP-type peroxidase and activity towards Kraft lignin and lignin model compounds. Arch. Biochem. Biophys. 594, 54–60. https://doi.org/10.1016/j.abb.2016.02.019.

Ramachandra, M., Crawford, D.L., Hertel, G., 1988. Characterization of an extracellular lignin peroxidase of the lignocellulolytic actinomycete *Streptomyces viridosporus*. Appl. Environ. Microbiol. 54, 3057–3063.

Ramalingam, P., Devi, V., 2017. Biodegradation and decolorization of azo dyes using marine bacteria. Int. J. Biotechnol. Res. 7, 1–12.

Roberts, J.N., Singh, R., Grigg, J.C., Murphy, M.E.P., Bugg, T.D.H., Eltis, L.D., 2011. Characterization of dye-decolorizing peroxidases from *Rhodococcus jostii* RHA1. Biochemistry 50, 5108–5119.

Sarkar, S., Banerjee, A., Halder, U., Biswas, R., Bandopadhyay, R., 2017. Degradation of synthetic azo dyes of textile industry: a sustainable approach using microbial enzymes. Water Conserv. Sci. Eng. 2, 121–131.

Shanmugam, B.K., Mahadevan, S., 2015. Metabolism and biotransformation of azo dye by bacterial consortium studied in a bioreaction calorimeter. Bioresour. Technol. 196, 500–508. https://doi.org/10.1016/j.biortech.2015.07. 108.

Song, L., Shao, Y., Ning, S., Tan, L., 2017. Performance of a newly isolated salt-tolerant yeast strain Pichia occidentalis G1 for degrading and detoxifying azo dyes. Bioresour. Technol. 233, 21–29. https://doi.org/10.1016/j.biortech.2017.02.065.

Sridhar, S., Chandra, J.H., 2014. Involvement of computational tools towards in-silico remediation-synthetic textile dyes interacting with azoreductase. Int. J. Chem. Res. 6, 4412–4416.

Srinivasan, S., Sadasivam, S.K., 2018. Exploring docking and aerobic-microaerophilic 570 biodegradation of textile azo dye by bacterial systems. J. Water Proc. Eng. 22, 180–191. https://doi.org/10.1016/j/jwpe.2018.02.004.

Tamboli, D., Kagalkar, A., Jadhav, M., Jadhav, J., Govindwar, S., 2010. Production of polyhydroxyhexadecanoic acid by using waste biomass of Sphingobacterium sp. ATM generated after degradation of textile dye Direct Red 5B. Bioresour. Technol. 101, 2421–2427. https://doi.org/10.1016/j.biortech.2009.11.094.

Tan, L., Ning, S., Zhang, X., Shi, S., 2013. Aerobic decolorization and degradation of azo dyes by growing cells of a newly isolated yeast Candida tropicalis TL-F1. Bioresour. Technol. 138, 307–313.

Weininger, D., 1988. SMILES, a chemical language and information system introduction to methodology and encoding rules. J. Chem. Inf. Comput. Sci. 28, 31–36.